

Variational Quantum Computation of Excited States

Oscar Higgott,¹ Daochen Wang,¹ and Stephen Brierley^{1,2}

¹*River Lane Research, Cambridge CB3 0GT, United Kingdom*

²*Department of Applied Mathematics and Theoretical Physics,
University of Cambridge, Cambridge CB3 0WA, United Kingdom*

The calculation of excited state energies of electronic structure Hamiltonians has many important applications, such as the calculation of optical spectra and reaction rates. While low-depth quantum algorithms, such as the variational quantum eigenvalue solver (VQE), have been used to determine ground state energies, methods for calculating excited states currently involve the implementation of high-depth controlled-unitaries or a large number of additional samples. Here we show how overlap estimation can be used to deflate eigenstates once they are found, enabling the calculation of excited state energies and their degeneracies. We propose an implementation that requires the same number of qubits as VQE and at most twice the circuit depth. Our method is robust to control errors, is compatible with error-mitigation strategies and can be implemented on near-term quantum computers.

I. INTRODUCTION

Eigenvalue problems are ubiquitous in almost all fields of science and engineering. Google’s PageRank algorithm alone has had a significant impact on modern society, and at its core solves an eigenvalue problem associated with a stochastic matrix describing the World Wide Web [1]. Another important example is Principal Component Analysis (PCA) [2, 3], that has widespread applications in bioinformatics, neuroscience, image processing and quantitative finance.

The time-independent Schrödinger equation provides yet another example of a fundamental eigenvalue problem. Its numerical solution enables properties of atoms, molecules and materials to be predicted, with far-reaching applications in materials design, drug discovery and fundamental science [4]. Characterisation of excited state energies of molecules is required to predict charge and energy transfer processes in photovoltaic materials, or to understand some chemical reactions, such as those that involve photodissociation. However, classical methods such as density functional theory are often unable to determine excited states, even for materials where ground state energy calculations are possible.

Quantum computers have the potential to solve these and other problems significantly faster than any known methods using classical computers [5–9]. However many quantum algorithms will require quantum error correction, limiting their usefulness in the near future [10]. Here we study hybrid quantum-classical algorithms, which dramatically reduce the required gate depth to run and somewhat mitigate errors, by closely integrating classical and quantum subroutines [11–18].

The Variational Quantum Eigensolver (VQE), introduced in Ref. [19], is the first algorithm designed to find the lowest eigenvalue of a Hamiltonian on near-term, non-fault-tolerant quantum computers. VQE is based on the variational principle, and utilises the fact that quantum computers can store quantum states using exponentially fewer resources than required classically. VQE uses pa-

rameterised quantum circuits to prepare trial wavefunctions and compute their energy, and a classical computer to find the parameters minimising this energy. The low circuit depth of VQE has led to hope that it may enable near-term quantum-enhanced computation.

Since its introduction, modifications have been suggested to enable VQE to find excited state energies: e.g. a folded spectrum method [19] which requires finding the expectation of the squared Hamiltonian with quadratically more terms, or symmetry-based methods which are non-systematic [11]. Such suggestions have been more recently superseded by two proposals: a method that minimises the von Neumann entropy [20] and the quantum subspace expansion method [21, 22]. However, the von Neumann entropy method (“WAVES”) requires a large number of high-depth controlled-unitaries, and the quantum subspace expansion method requires a large number of additional samples compared to VQE and introduces a new approximation.

Our algorithm extends VQE to systematically find excited states at almost no extra cost. We achieve this by adding “overlap” terms onto the optimisation function in order to exploit the fact that Hermitian matrices admit a complete set of orthogonal eigenvectors. Exploiting further the fact that VQE retains the classical parameters of ansatz states that enable their re-preparation, low-depth quantum circuits can then be readily used to calculate these overlap terms.

II. VARIATIONAL QUANTUM DEFLATION ALGORITHM

In VQE, the real parameters $\vec{\lambda}$ for the ansatz state $|\psi(\vec{\lambda})\rangle$ are classically optimised with respect to the expectation value:

$$E(\vec{\lambda}) := \langle \psi(\vec{\lambda}) | H | \psi(\vec{\lambda}) \rangle = \sum_j a_j \langle \psi(\vec{\lambda}) | P_j | \psi(\vec{\lambda}) \rangle, \quad (1)$$

of the Hamiltonian $H = \sum c_j P_j$, computed using a low-depth quantum circuit. As a result of the variational

principle, finding the global minimum of $E(\vec{\lambda})$ is equivalent to finding the ground state energy of H . VQE has been implemented on many experimental platforms, and has been shown to be more resilient to control errors than the quantum phase estimation algorithm [23].

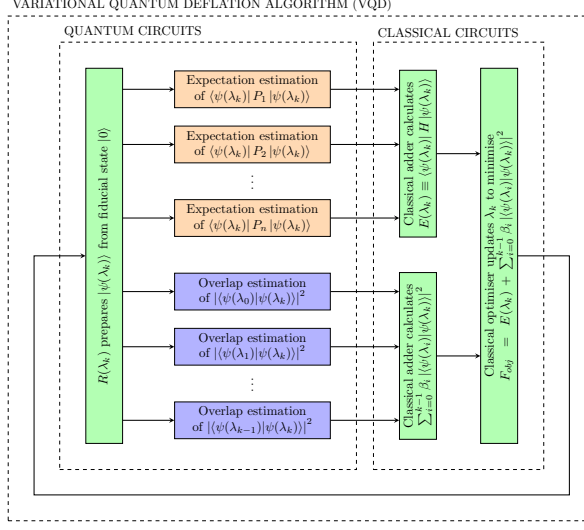


FIG. 1. A schematic of our variational quantum deflation method for finding the k -th excited state of a Hamiltonian H .

Our method extends VQE to calculate the k -th excited state by instead optimising the parameters $\vec{\lambda}_k$ for the ansatz state $|\psi(\vec{\lambda}_k)\rangle$ such that the cost function:

$$F(\vec{\lambda}_k) := \langle\psi(\vec{\lambda}_k)| H |\psi(\vec{\lambda}_k)\rangle + \sum_{i=0}^{k-1} \beta_i \left| \langle\psi(\vec{\lambda}_k)|\psi(\vec{\lambda}_i)\rangle \right|^2, \quad (2)$$

is minimised. This can be seen as minimising $E(\vec{\lambda}_k)$ subject to the constraint that $|\psi(\vec{\lambda}_k)\rangle$ is orthogonal to the states $|\psi(\vec{\lambda}_0)\rangle, \dots, |\psi(\vec{\lambda}_{k-1})\rangle$. In the next section, we show how choosing sufficiently large $\beta_0, \dots, \beta_{k-1}$ means the minimum of $F(\vec{\lambda}_k)$ is guaranteed to be the energy of the k -th state.

While the first term in Eq. (2) is $E(\vec{\lambda}_k)$, and can be computed using the same quantum circuits as used for VQE, the second term is a sum of overlaps of the ansatz state with states 0 to $k-1$, and can be computed efficiently on a quantum computer using one of the methods given in Section IV.

Note that evaluating Eq. (2) requires knowledge of $\vec{\lambda}_0, \dots, \vec{\lambda}_{k-1}$ and so an iterative procedure is required to calculate the k -th eigenvalue. First, $\vec{\lambda}_0$ is calculated using VQE by minimising E in Eq. (1). Then, $\vec{\lambda}_1$ is calculated by minimising F in Eq. (2) for $k=1$, after which $\vec{\lambda}_2$ can be determined using the same procedure with the known $\vec{\lambda}_0$ and $\vec{\lambda}_1$, and so on until $\vec{\lambda}_k$ is determined.

A schematic of our VQD algorithm is shown in Fig. 1. An initial guess of $\vec{\lambda}_k$ is used to generate a state prepara-

tion circuit $R(\vec{\lambda}_k)$ that prepares the state $|\psi(\vec{\lambda}_k)\rangle$ when applied to the fiducial state $|0\rangle$. This circuit is used repeatedly to compute each of the expectation values $\langle\psi(\vec{\lambda}_k)| P_j |\psi(\vec{\lambda}_k)\rangle$ (see Refs. [13, 19]) and overlap terms $|\langle\psi(\vec{\lambda}_k)|\psi(\vec{\lambda}_i)\rangle|^2$ for $i < k$. The overlap terms are computed to precision ϵ using circuits described in Section IV, Appendix A or Appendix B.

A classical computer then uses the results of these quantum computations to calculate the objective function $F(\vec{\lambda}_k)$ of Eq. (2) and update $\vec{\lambda}_k$ using a classical optimiser. The new $\vec{\lambda}_k$ is then used to prepare a new ansatz state on the quantum computer, and the whole process is repeated until some stopping criterion is reached.

III. OVERLAP WEIGHTING

An equivalent viewpoint of our optimisation procedure is that we are finding the ground state of the effective Hamiltonian at stage k :

$$H_k := H + \sum_{i=0}^{k-1} \beta_i |i\rangle\langle i|, \quad (3)$$

where $|i\rangle$ is the (previously found) i -th eigenstate of H with energy $E_i := \langle i|H|i\rangle$ [24]. It can be easily verified that for an arbitrary state $|\psi\rangle := \sum a_i |i\rangle$:

$$\langle\psi| H_k |\psi\rangle = \sum_{i=0}^{k-1} |a_i|^2 (E_i + \beta_i) + \sum_{i=k}^{d-1} |a_i|^2 E_i,$$

where d is the total number of eigenvectors of H .

Therefore, to guarantee a minimum at E_k , it suffices to choose $\beta_i > E_k - E_i$. Since $\Delta := E_{d-1} - E_0 \geq E_k - E_i$, it suffices to possess an accurate estimate of Δ , e.g. by using VQE to find E_0 and then E_{d-1} (using the Hamiltonian $-H$ to find the latter). When we readily have a specification of $H = \sum c_j P_j$ as a linear combination of Pauli matrices, e.g. when H is the electronic structure Hamiltonian, then we have the upper bound $\Delta \leq 2\|H\| \leq 2\sum |c_j|$. In this case, we can readily choose β_i to guarantee the validity of our procedure.

Choosing valid β_i can also be self-correcting. For example, if we incorrectly chose $\beta_i = F - E_i \leq E_k - E_i$ for all i , we will discover that we have set β_i too small since we will eventually find a minimum at $F(\vec{\lambda}_k) = F$. However, by repeating the algorithm with a larger F until an energy strictly less than F is found (doubling F each time, say), we can pick a large enough F after $O(\log(E_k - E_0))$ runs of the algorithm.

IV. LOW-DEPTH IMPLEMENTATIONS

A low-depth method for overlap estimation, proposed in Ref. [25], can be seen by writing the overlap

$|\langle \psi(\vec{\lambda}_i) | \psi(\vec{\lambda}_k) \rangle|^2$ as $|\langle 0 | R(\vec{\lambda}_i)^\dagger R(\vec{\lambda}_k) | 0 \rangle|^2$. We can prepare the state $R(\vec{\lambda}_i)^\dagger R(\vec{\lambda}_k) | 0 \rangle$ using the trial state preparation circuit followed by the inverse of the preparation circuit for the i -th previously-computed state. The overlap is then estimated to precision ϵ by the fraction of all-zero bitstrings when measuring this state $O(1/\epsilon^2)$ times in the computational basis.

This method requires knowing the inverse of the preparation circuit for each previously-computed state, $R(\vec{\lambda}_i)^\dagger$. While this inverse is often known in theory by inverting gates in a decomposition of the original preparation circuit, device errors may mean that the implementation is inaccurate in practice. If we define $\vec{\lambda}_i^*$ to be the optimal parameters originally found to prepare the i -th state $R(\vec{\lambda}_i^*) | 0 \rangle$ using VQD, then its inverse can be found by fixing $\vec{\lambda}_i^*$ and varying the trial state parameters $\vec{\lambda}_i$ such that the overlap $|\langle 0 | R(\vec{\lambda}_i)^\dagger R(\vec{\lambda}_i^*) | 0 \rangle|^2$ is maximised. This technique enables VQD to retain the robustness to control errors that is characteristic of VQE [23].

This implementation of VQD requires the same number of qubits as VQE and around twice the circuit depth. In Appendix A, we describe an alternative method which uses the destructive SWAP test and requires almost the same circuit depth as VQE but twice the number of qubits. If a larger gate-depth is available, then the overlap estimation circuits in Appendix B can be used in conjunction with α -QPE [13] to reduce the total runtime of overlap estimation from $O(\frac{1}{\epsilon^2})$ up to $O(\frac{1}{\epsilon})$.

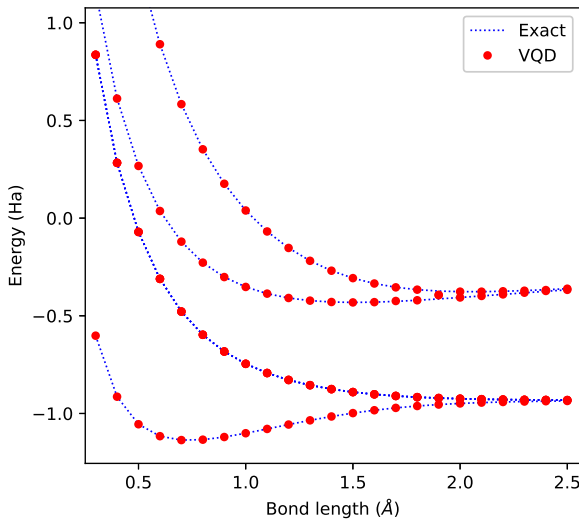


FIG. 2. All ground and excited state energy levels of H_2 , calculated in the STO-3G basis by exact diagonalisation (blue dotted line) and our variational quantum deflation (VQD) method (red filled circles) over a range of internuclear separations.

V. NUMERICAL SIMULATION: H_2

We simulated VQD on H_2 in the STO-3G basis for a range of internuclear separations and compared it to exact diagonalisation, as shown in Fig. 2. Using $\beta_i = 3 \text{ Ha}$ for all i and a unitary coupled cluster singles and doubles (UCCSD) ansatz, the median error of our method is less than $4 \times 10^{-6} \text{ Ha}$ for all energy levels, significantly better than chemical accuracy ($1.6 \times 10^{-3} \text{ Ha}$). Our method finds all 6 eigenstates systematically, including all those in the 3-dimensional degenerate subspace spanned by the 1st, 2nd and 3rd excited states. The ability to find degenerate states is another key advantage of our method; the folded spectrum and WAVES methods rely on the energies of states to differentiate between them and have no systematic way of determining the degeneracy of the eigenvalues. Further discussion of our simulation, including optimiser and ansatz used, can be found in Appendix C.

VI. CHOICE OF EFFECTIVE HAMILTONIAN

The form of our effective Hamiltonian in Eq. (3) is only one choice within the broad category of deflation methods. Such methods are typically employed to find eigenvalues and eigenvectors of positive semi-definite matrices, often covariance matrices in the context of PCA, starting from the largest eigenvalues.

To make direct use of deflation methods for positive semi-definite matrices, note that the Hamiltonian $H' := -H + E'$ for some $E' \geq E_{d-1}$, e.g. $E' = \|H\|$, is positive semi-definite. Under this transformation, we find that Hotelling's deflation corresponds to our method and would set $\beta_i = E' - E_i$ in Eq. (3).

Other deflation methods exist such as projection deflation or Schur complement deflation which are designed to address the problem of not obtaining true eigenstates at each stage. These two methods, in contrast to Hotelling's, ensure that the true ground state of the effective Hamiltonian at each stage does not overlap with the previously found eigenstate estimates irrespective of their accuracy. Empirically, these two methods have been found to perform better than Hotelling's in the context of PCA on some datasets [26].

For example, in projection deflation, the effective Hamiltonian at stage k is defined as:

$$H_k = A_k^\dagger (H - E') A_k, \quad (4)$$

where:

$$A_k := \prod_{i=0}^{k-1} (1 - |i\rangle \langle i|) \approx 1 - \sum_{i=0}^{k-1} |i\rangle \langle i|, \quad (5)$$

and the last approximation holds when the previously found eigenvectors $|i\rangle$ are truly orthogonal.

With this approximation, writing H again as a linear combination of Pauli matrices P_j , the value of $\langle \psi | H_k | \psi \rangle$ for an ansatz $|\psi\rangle$ is a linear combination of terms of forms: $\langle \psi | P_j | \psi \rangle$, $|\langle \psi | i \rangle|^2$ as in Hotelling's deflation, but now additionally $\langle \psi | i \rangle$, $\langle \psi | P_j | i \rangle$ and $\langle i | P_j | l \rangle$ (for $i, l < k$).

Without this approximation, we also need to calculate $\langle i | l \rangle$. The important point now is that all these additional terms can still be quantum computed, e.g. following the method in Ref. [27] which is outlined in Appendix B.

[1] L. Page, S. Brin, R. Motwani, T. Winograd, *The PageRank citation ranking: Bringing order to the web.*, Tech. Rep., Stanford InfoLab, **1999**.

[2] K. Pearson, *The London, Edinburgh, and Dublin Philosophical Magazine and Journal of Science* **1901**, 2, 559–572.

[3] H. Hotelling, *Journal of educational psychology* **1933**, 24, 417.

[4] A. Szabo, N. S. Ostlund, *Modern quantum chemistry: introduction to advanced electronic structure theory*, Courier Corporation, **2012**.

[5] S. Lloyd, M. Mohseni, P. Rebentrost, *Nature Physics* **2014**, 10, 631.

[6] S. Garnerone, P. Zanardi, D. A. Lidar, *Physical review letters* **2012**, 108, 230506.

[7] P. W. Shor, *SIAM review* **1999**, 41, 303–332.

[8] L. K. Grover in *Proceedings of the twenty-eighth annual ACM symposium on Theory of computing*, ACM, pp. 212–219.

[9] A. Aspuru-Guzik, A. D. Dutoi, P. J. Love, M. Head-Gordon, *Science* **2005**, 309, 1704–1707.

[10] J. Preskill, *arXiv:1801.00862v2*.

[11] J. R. McClean, J. Romero, R. Babbush, A. Aspuru-Guzik, *New Journal of Physics* **2016**, 18, 023023.

[12] E. Farhi, J. Goldstone, S. Gutmann, *arXiv preprint arXiv:1411.4028* **2014**.

[13] D. Wang, O. Higgott, S. Brierley, *arXiv preprint arXiv:1802.00171* **2018**.

[14] P. D. Johnson, J. Romero, J. Olson, Y. Cao, A. Aspuru-Guzik, *arXiv preprint arXiv:1711.02249* **2017**.

[15] N. Moll, P. Barkoutsos, L. S. Bishop, J. M. Chow, A. Cross, D. J. Egger, S. Filipp, A. Fuhrer, J. M. Gambetta, M. Ganzhorn, et al., *arXiv preprint arXiv:1710.01022* **2017**.

[16] M. Benedetti, D. Garcia-Pintos, Y. Nam, A. Perdomo-Ortiz, *arXiv preprint arXiv:1801.07686* **2018**.

[17] S. McArdle, S. Endo, Y. Li, S. Benjamin, X. Yuan, *arXiv preprint arXiv:1804.03023* **2018**.

[18] S. Endo, T. Jones, S. McArdle, X. Yuan, S. Benjamin, *arXiv preprint arXiv:1806.05707* **2018**.

[19] A. Peruzzo, J. McClean, P. Shadbolt, M.-H. Yung, X.-Q. Zhou, P. J. Love, A. Aspuru-Guzik, J. L. O'brien, *Nature communications* **2014**, 5.

[20] R. Santagati, J. Wang, A. A. Gentile, S. Paesani, N. Wiebe, J. R. McClean, S. Morley-Short, P. J. Shadbolt, D. Bonneau, J. W. Silverstone, et al., *Science advances* **2018**, 4, eaap9646.

[21] J. R. McClean, M. E. Kimchi-Schwartz, J. Carter, W. A. de Jong, *Physical Review A* **2017**, 95, 042308.

[22] J. Colless, V. Ramasesh, D. Dahlen, M. Blok, M. Kimchi-Schwartz, J. McClean, J. Carter, W. De Jong, I. Siddiqi, *Physical Review X* **2018**, 8, 011021.

[23] P. O'Malley, R. Babbush, I. Kivlichan, J. Romero, J. McClean, R. Barends, J. Kelly, P. Roushan, A. Tranter, N. Ding, et al., *Physical Review X* **2016**, 6, 031007.

[24] We assume these are true eigenstates with possibly non-distinct energies.

[25] V. Havlicek, A. D. Córcoles, K. Temme, A. W. Harrow, J. M. Chow, J. M. Gambetta, *arXiv preprint arXiv:1804.11326* **2018**.

[26] L. W. Mackey **2009**, 1017–1024.

[27] E. Knill, G. Ortiz, R. D. Somma, *Phys. Rev. A* **2007**, 75, 012328.

[28] J. C. Garcia-Escartin, P. Chamorro-Posada, *Physical Review A* **2013**, 87, 052330.

[29] L. Cincio, Y. Subaşı, A. T. Sornborger, P. J. Coles, *arXiv preprint arXiv:1803.04114* **2018**.

[30] I. D. Kivlichan, J. McClean, N. Wiebe, C. Gidney, A. Aspuru-Guzik, G. K.-L. Chan, R. Babbush, *Physical review letters* **2018**, 120, 110501.

[31] J. Romero, J. P. Olson, A. Aspuru-Guzik, *Quantum Science and Technology* **2017**, 2, 045001.

[32] J. Romero, R. Babbush, J. R. McClean, C. Hempel, P. J. Love, A. Aspuru-Guzik, *arXiv preprint arXiv:1701.02691* **2017**.

[33] D. S. Steiger, T. Häner, M. Troyer, *Quantum* **2018**, 2, 49.

[34] J. R. McClean, I. D. Kivlichan, D. S. Steiger, Y. Cao, E. S. Fried, C. Gidney, T. Häner, V. Havlicek, Z. Jiang, M. Neeley, et al., *arXiv preprint arXiv:1710.07629* **2017**.

[35] I. G. Ryabinkin, S. N. Genin, A. F. Izmaylov, *arXiv preprint arXiv:1806.00461* **2018**.

[36] S. McArdle, X. Yuan, S. Benjamin, *arXiv preprint arXiv:1807.02467* **2018**.

[37] S. Endo, S. C. Benjamin, Y. Li, *arXiv preprint arXiv:1712.09271* **2017**.

[38] K. Temme, S. Bravyi, J. M. Gambetta, *Physical review letters* **2017**, 119, 180509.

Appendix A: Destructive SWAP Test

The SWAP test enables the overlap $|\langle \phi | \psi \rangle|^2$ of two states $|\psi\rangle$ and $|\phi\rangle$ to be determined to precision ϵ using $O(1/\epsilon^2)$ repeated measurements after applying a circuit to a quantum register in the state $|\psi\rangle \otimes |\phi\rangle$. While the original SWAP test acting on two N -qubit states required an ancilla and a controlled-SWAP gate, leading to a $2N + 1$ -qubit circuit with depth $O(N)$, it was shown in Refs. [28, 29] that the same outcome distribution can be attained more efficiently without an ancilla, using parallel Bell-basis measurements and classical logic. This so-called ‘‘destructive SWAP test’’ (shown in Fig. 3) requires just $2N$ qubits and depth $O(1)$, achieving significant savings compared to the original SWAP test.

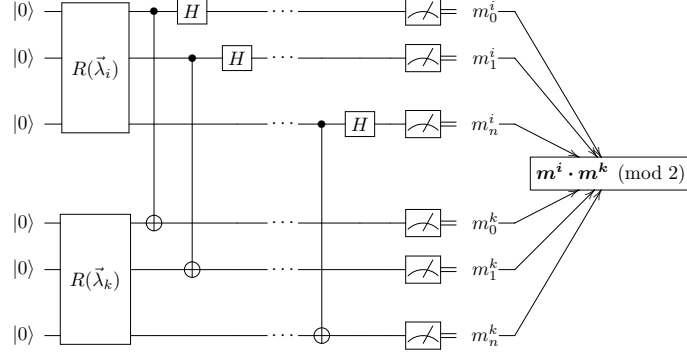


FIG. 3. The N -qubit generalisation of the destructive SWAP test as applied to two ansatz states $|\psi(\vec{\lambda}_i)\rangle$ and $|\psi(\vec{\lambda}_k)\rangle$, prepared using state preparation circuits $R(\vec{\lambda}_i)$ and $R(\vec{\lambda}_k)$ respectively.

If the ansatz used can be implemented on a linear chain of qubits with nearest neighbour connectivity, e.g. parameterised adiabatic state preparation using the fermionic SWAP network Trotter step [30], then the SWAP test to compare two ansatz states can be implemented on a $N \times 2$ nearest-neighbour grid quantum computer architecture with a depth-one circuit that is subgraph isomorphic to the architecture (i.e. no routing of quantum information required). This implementation makes the assumption that the same ansatz state can be prepared with the same parameters on two separate registers of qubits. If this cannot be assumed (e.g. if qubit errors are inhomogeneous), then the SWAP test can be used to ‘‘copy’’ the state from the first register to the second register, by maximising the overlap of the two states, with the parameters of the state on the second register allowed to vary. This technique allows the SWAP test implementation of VQD to maintain robustness to control errors.

We note that the low-depth implementations of overlap estimation we use can be utilised to simplify other recently proposed quantum algorithms. For example, the method for overlap described in Section IV can replace the ancilla-based SWAP test in the quantum autoencoder [31]. With this simplification, the ancilla as well as the qubit register containing the reference state $|a\rangle$ can be removed, and the autoencoder (for $|a\rangle=|0\rangle$) corresponds exactly to maximising the fraction of all-zero bitstrings after measurements in the computational basis (and hence enforcing symmetry in their Fig. 1b diagram).

Appendix B: Overlap Estimation Circuits

To calculate $\omega := \langle \psi | P | \phi \rangle$ for any unitary P , we may perform quantum phase estimation (QPE) on the operators U_0 , U_1 and U_2 with input states $|\psi\rangle$, $|+\psi\rangle$, $|-\psi\rangle$ as depicted in Figs. 4, 5, 6 respectively. These respectively yield the values: $b_0 := |\omega|$, $b_1 := |1 + \omega|/2$ and $b_2 := |1 - i\omega|/2$. Then we can find w via $\text{Re}(\omega) = (4b_1^2 - b_0 - 1)/2$ and $\text{Im}(\omega) = (4b_2^2 - b_0 - 1)/2$.

Alternatively, a variable depth version of QPE may be used when quantum coherence is lacking. In Ref. [13], we derived the scaling of one such QPE that requires $O(1/\epsilon^{2(1-\alpha)})$ measurements and maximum circuit depth of $O(1/\epsilon^\alpha)$. When $\alpha = 0$, we would be performing simple statistical sampling on a biased coin with head probabilities b_0^2 , b_1^2 , b_2^2 .

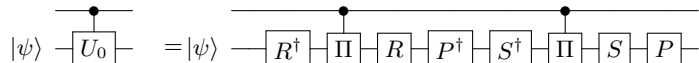


FIG. 4. The eigenphases $\pm\alpha_0$ of U_0 on $|\psi\rangle$ can be used to calculate $b_0 := \cos(\pm\alpha_0) = |\langle \psi | P | \phi \rangle|$. P is any unitary, R and S denote preparation circuits of $|\psi\rangle$ and $|\phi\rangle$ respectively, and Π denotes $1 - 2|0\rangle\langle 0|$.

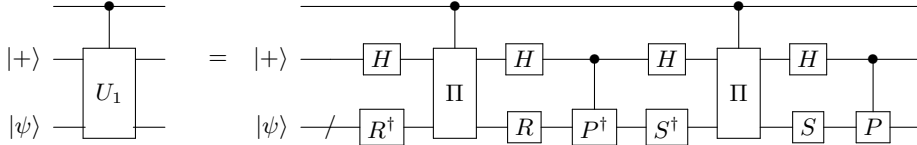


FIG. 5. The eigenphases $\pm\alpha_1$ of U_1 on $|+\psi\rangle$ can be used to calculate $b_1 := \cos(\pm\alpha_1/2) = \left| \frac{1+\langle\psi|P|\phi\rangle}{2} \right|$.

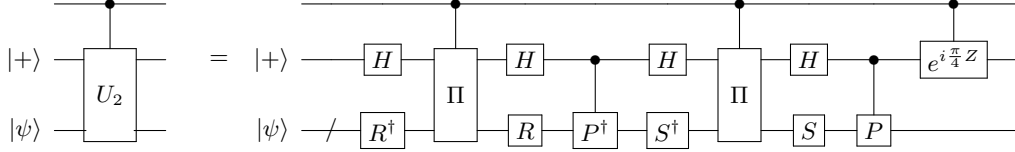


FIG. 6. The eigenphases $\pm\alpha_2$ of U_2 on $|+\psi\rangle$ can be used to determine $b_2 := \cos(\pm\alpha_2/2) = \left| \frac{1-i\langle\psi|P|\phi\rangle}{2} \right|$.

Appendix C: Methods for Numerical Simulation

The standard UCCSD ansatz [32] is defined relative to a reference state $|\psi_0\rangle$ by:

$$|\psi\rangle = e^{T-T^\dagger} |\psi_0\rangle,$$

where $T := T_1 + T_2$ with:

$$\begin{aligned} T_1 &:= \sum_{\substack{i \in \text{occ} \\ l \in \text{vir}}} t_i^l a_m^\dagger a_i, \\ T_2 &:= \sum_{\substack{i,j \in \text{occ} \\ l,k \in \text{vir}}} t_{ij}^{lk} a_l^\dagger a_k^\dagger a_i a_j, \end{aligned}$$

for some parameters t_i^l , $t_{ij}^{lk} \in \mathbb{R}$ and occ and vir are the sets of occupied and virtual orbitals of $|\psi_0\rangle$.

The UCCSD ansatz we used has $|\psi_0\rangle = |\text{HF}\rangle$ set to the Hartree-Fock state but with the redefinitions:

$$\begin{aligned} T_1 &:= \sum_{\substack{\text{occ} \\ \text{vir}}} \sum_{\substack{i \in \text{occ} \\ l \in \text{vir}}} t_i^l a_m^\dagger a_i, \\ T_2 &:= \sum_{\substack{\text{occ} \\ \text{vir}}} \sum_{\substack{i,j \in \text{occ} \\ l,k \in \text{vir}}} t_{ij}^{lk} a_l^\dagger a_k^\dagger a_i a_j, \end{aligned}$$

where the first sums are now over all possible sets of occupied and virtual orbitals with 2 electrons.

Since we are only interested in the parameterisation of $T - T^\dagger$, and fermionic operators obey the anti-commutation relations:

$$\{a_j, a_k\} = 0, \quad \{a_j^\dagger, a_k^\dagger\} = 0, \quad \{a_j, a_k^\dagger\} = \delta_j^k,$$

it can be directly verified that there are only 6 and 3 independent parameters for T_1 (e.g. $t_0^1, t_0^2, t_0^3, t_1^2, t_1^3, t_2^3$) and T_2 (e.g. $t_{01}^{23}, t_{02}^{13}, t_{03}^{12}$) respectively.

The results in Fig. 2 were simulated using ProjectQ and FermiLib [33, 34]. A tolerance of 10^{-2} was used with a Nelder-Mead optimiser (xatol=fatol= 10^{-2} , as implemented in the scipy Python scientific library), and the best of two consecutive (randomly initialised) runs was used for each bond length and energy level. We note that other optimisers, such as LGO, have been shown to offer improved performance in VQE [11], and possible further work includes analysis of alternative optimisation strategies in the context VQD.

We also note that the overlap terms $|\langle\psi(\vec{\lambda}_k)|\psi(\vec{\lambda}_i)\rangle|^2$ in Eq. (2) of the state k with a known state i are similar to the overlap terms $|\langle\psi(\vec{\lambda}_s^t)|\psi(\vec{\lambda}_i)\rangle|^2$ of the same known state i with another previously-computed state s (where $i < s < k$) in the t -th iteration of the VQD optimisation procedure used to compute that state. It may therefore be advantageous to cache the outputs of these $|\langle\psi(\vec{\lambda}_s^t)|\psi(\vec{\lambda}_i)\rangle|^2$ terms, and use them to inform and improve the optimisation procedure for the k -th state, hopefully reducing the number of optimisation steps and quantum circuits required.

Appendix D: Symmetry Constraints

It is often the case that the Hilbert space of the Hamiltonian being considered is larger than the Hilbert space relevant to the particular problem of interest. For example, consider the electronic structure Hamiltonian in second-quantized form,

$$H = \sum_{ij} h_{ij} a_i^\dagger a_j + \sum_{ijkl} h_{ijkl} a_i^\dagger a_j^\dagger a_k a_l, \quad (\text{D1})$$

where a_i^\dagger and a_i are the fermionic creation and annihilation operators for an electron in the i -th spin orbital, and where the coefficients h_{ij} and h_{ijkl} denote the one- and two-electron integrals, respectively. After the Hamiltonian is transformed through the Jordan-Wigner or Bravyi-Kitaev transformation, converting creation and annihilation operators into qubit operators, the dimension of the Hilbert space remains 2^N , where N is the number of spin orbitals. However, if one is interested only in states with a particular symmetry, the dimension of the Hilbert space restricted only to these states can be much smaller, e.g. $\binom{N}{\eta} = O(N^\eta)$ instead of 2^N if only η -electron states are of interest.

If we wish to apply VQD to find excited states of a molecular Hamiltonian with a particular symmetry, it is necessary that the ansatz state for a desired excited state, at the global minimum of Eq. (2), be contained entirely within the restricted Hilbert space of interest. One way of ensuring this is to use an ansatz that always conserves the correct symmetry. For example, the fermionic unitary coupled cluster ansatz we use in Section V conserves the desired number of electrons ($\eta = 2$) of neutral molecular Hydrogen for all input parameters.

Alternatively, penalty terms can be included in the objective function such that the ansatz state has the desired symmetry at the global minimum of the objective function [11, 35]. This leads to a modified objective function

$$F_C(\vec{\lambda}_k) := F(\vec{\lambda}_k) + \sum_i \mu_i [\langle \psi(\vec{\lambda}_k) | \hat{C}_i | \psi(\vec{\lambda}_k) \rangle - c_i]^2 \quad (\text{D2})$$

where \hat{C}_i are symmetry constraining operators (e.g. \hat{N}_e , \hat{S}^2 , \hat{S}_z) and c_i are constants corresponding to their desired expectation values.

Clearly, by incorporating any of these techniques, we can find the excited states of a Hamiltonian constrained to any particular symmetry of interest.

Appendix E: Error Mitigation

In Refs. [35, 36], an error-mitigating post-processing procedure was introduced that uses the operators \hat{C}_i (defined in Appendix D) to detect and discard all measurements that violate a required symmetry for energy expectation circuits in VQE-type algorithms. This procedure can produce more accurate expectation values in the presence of bit-flip errors and some combinations of two-qubit errors.

After the first version of this paper was released, Ref. [18] incorporated our VQD technique to calculate excited states using imaginary time evolution. The authors also proposed a method to detect symmetry-breaking errors when using the ancilla-based SWAP-test, by performing symmetry measurements on the ansatz registers while measuring the overlap with the ancilla. However, using the low-depth overlap estimation circuit given in Section IV, we can detect and discard any error that does not commute with a symmetry operator \hat{C}_i using classical post-processing alone, provided that \hat{C}_i is diagonal in the computational basis and commutes with the ansatz. In the Jordan-Wigner and Bravyi-Kitaev encodings, the operators for the number of electrons \hat{N}_e , spin up electrons \hat{N}_\uparrow and spin down electrons \hat{N}_\downarrow are diagonal in the computational basis, allowing these quantities to be computed classically in post-processing for both encodings. For example, starting from $|0\rangle$, the UCC ansatz is prepared by $R_{\text{UCC}}(\vec{\lambda}) = V(\vec{\lambda})R_{\text{HF}}$, where R_{HF} prepares the Hartree-Fock state $|\text{HF}\rangle$ and $V := e^{T-T^\dagger}$ is the UCC operator. Now, rather than measuring the fraction of all-zero bitstrings after performing $R_{\text{UCC}}(\vec{\lambda}_i)^\dagger R_{\text{UCC}}(\vec{\lambda}_k) |0\rangle = R_{\text{HF}}^\dagger V(\vec{\lambda}_i)^\dagger V(\vec{\lambda}_k) R_{\text{HF}} |0\rangle$, we can instead measure the fraction of bitstrings corresponding to $|\text{HF}\rangle$ after performing $V(\vec{\lambda}_i)^\dagger V(\vec{\lambda}_k) R_{\text{HF}} |0\rangle$. Since V conserves electron number, we know that all measured bitstrings that do not correspond to the correct electron number can be discarded as per the post-processing procedure. This method for error-mitigated overlap estimation is therefore substantially more efficient than the ancilla-based method proposed in Ref. [18] if \hat{C}_i is diagonal in the computational basis. We also note that the error-mitigation techniques proposed in Refs. [37, 38] can be readily applied to our algorithm.

Appendix F: Circuit Simplifications

While this method requires just twice the gate depth of normal VQE we note that, for some Hamiltonians and types of ansatz, the circuit $R(\vec{\lambda}_i)^\dagger R(\vec{\lambda}_k)$ can be simplified further. For example, since not all gates in $R(\vec{\lambda}_i)^\dagger$ and $R(\vec{\lambda}_k)$ are parameterised, we would expect some gates in $R(\vec{\lambda}_i)^\dagger$ to cancel with some gates in $R(\vec{\lambda}_k)$. Furthermore, rather than measuring the fraction of all-zero bitstrings at the end of the computation, we can measure at the earliest point in the circuit $R(\vec{\lambda}_i)^\dagger R(\vec{\lambda}_k)$ where we know that the Born probability of measuring a particular bitstring exactly corresponds to the overlap of the ansatz state $R(\vec{\lambda}_k) |0\rangle$ with the state $R(\vec{\lambda}_i) |0\rangle$. This allows R_{HF}^\dagger (defined in Appendix E) to be removed if the UCC ansatz is used, and allows $R(\vec{\lambda}_i)^\dagger$ to be removed if the state $|i\rangle$ is found to be a computational basis state.